The Ground and Valence Excited States of GaBr: A MR-CISD+*Q* Study

Xinzheng Yang, Meirong Lin,* and Baozheng Zhang

Institute of Modern Optics, Optoelectronic Information Science and Technology Laboratory, EMC, Nankai University, Tianjin 300071, P. R. China

Received: January 11, 2004; In Final Form: March 2, 2004

Ab initio calculations on the ground and valence excited states of the GaBr molecule have been performed by using the entirely uncontracted all-electronic aug-cc-pVQZ basis sets and the internally contracted multireference singles and doubles configuration interaction method with Davidson size-extensivity correction and Douglas-Kroll scalar relativistic correction. The potential energy curves of all valence states and the spectroscopic constants of bound states are fitted. It is the first time that the entire 23 Ω states generated from the 12 Λ−S states of the GaBr molecule are studied in a theoretical way. Calculation results well reproduce most of the experimental data. The effects of the spin−orbit coupling and the avoided crossing rule between Ω states of the same symmetry are analyzed. The observed diffuse absorption bands near 36000 cm^{-1} can be contributed to the transitions from the C1(II) and other higher shallow potential well excited states, lying at the region of about 34000−38000 cm^{-1}, to the ground state. The transition properties of the $A^3\Pi_{0+}$ and $B^3\Pi_1$ states to the ground-state transitions are predicted for the first time, including the transition dipole moments, the Franck−Condon factors and the radiative lifetimes. The lifetime of the $A^3\Pi_{0+}$ state of the GaBr molecule is of the order of milliseconds, while that of the $B^3\Pi_1$ state is of the order of microseconds.

1. Introduction

Gallium monohalides have been attracting interest in their unique physical and chemical properties for a long time. They have been playing important roles in the development of new semiconductor devices in high frequency and in optoelectronic applications. In chemical vapor deposition techniques such as the Effer process,[1] gallium monohalides act as gas-phase transporters of semiconductor materials.[2−4] In a word, they have been of great value in searching for new laser media and semiconductors. There are many experimental and theoretical studies on the ground and low-lying electronic states of gallium monohalides, which have extended and deepened the comprehension of the properties of the electronic states of these molecules.

The first spectrum of GaBr was observed by Petrikalm and Hochberg[5] in absorption. Miescher and Werhli[6,7] studied the GaCl, GaBr, and GaI spectra and attributed the observed bands of GaBr to two electronic transitions. The bands in the region of 260−300 nm were attributed to the $C^1\Pi-X^1\Sigma^+$ transition system, the bands in the region of 340−360 nm were attributed to the $^3\Pi-X^1\Sigma^+$ transition (with two subsystems, $A^3\Pi_{0+}-X^1\Sigma^+$ and $B^3\Pi_1-X^1\Sigma^+$), and vibrational constants were determined. Subsequently, Barret and Mandel[8] observed the microwave rotational spectra of GaBr. Bulewicz et al.[9] and Barrow[10] reported the dissociation energy of GaBr. Savithry et al.[11] reported the emission band spectrum of GaBr in the region 340−370 nm. Most of these early studies had been summarized by Herzberg.[12] In recent decades, Nair et al.[13] measured the millimeter-wave rotational spectrum and molecular constants of GaBr. Burnecka et al.[14−17] measured the rotational structure of the $A^3\Pi_{0+}-X^1\Sigma^+$ and $B^3\Pi_1-X^1\Sigma^+$ transition systems and revised the exact vibrational constants of the A, B, and X states of GaBr. Grabandt et al.[18] measured and calculated the ionization energy of GaBr by using He(I) photoelectron spectroscopy and the Hartree−Fock−Slater method, respectively. Venkatasubramanian et al.[19] reported new visible emission spectra of GaBr, GaCl and InCl and forecasted the prospects of these molecules as an efficient excimer laser system. It's obvious that most of these experimental studies were focused on the ground and the low-lying $A^3\Pi_{0+}$ and $B^3\Pi_1$ excited states. Only diffuse absorption bands at about the 36000 cm^{-1} position indicate the existence of the $C^1\Pi_1$ state and nearby higher excited states.[6,7]

With the development of ab initio methods and computer technology, some calculations on the electronic state structures of GaBr have been reported in recent years.[20−23] However, most of these theoretical studies focused on the ground state, and none of these previous calculations had included the effect of spin−orbit coupling (SOC). It's well known that the SOC plays an important role in the spectroscopy and dynamics of molecules, even in the light molecules that contain only atoms of the first row of the periodic table. For instance, coupling of excited states of different spin multiplicities in regions where the corresponding potentials are nearly degenerate can lead to predissociation. Experimental data show that the spin−orbit splitting energy between the $A^3\Pi_{0+}$ and $B^3\Pi_1$ states of GaBr is greater than 370 cm^{-1},[12] and the splitting energies of the ground ^2P states of Ga and Br atoms are 826.24 cm^{-1} and 3685 cm^{-1},[24] respectively. These results mean that the SOC effect will strongly affect the shapes of potential energy curves (PECs) and the dissociation energy of the GaBr molecule. Besides being heavy elements, the relativistic effects of gallium and bromine atoms are expected to be very important. Therefore, both the SOC and the scalar relativistic correction have to be included in calculation, to compare with the experimental and theoretical data.

Since no generally applicable multireference coupled cluster (MR-CC) methods have been available up to now, multirefer-

* Corresponding author. E-mail: linzh@nankai.edu.cn, Tel: +86-22-23501554, Fax: +86-22-23502275.

10.1021/jp049868s CCC: $27.50
Published on Web 04/15/2004

ence configuration interaction (MRCI) methods have played an important role for the description of potential energy surfaces of both ground and excited states. Usually, for a correct description of excited states, the multiconfiguration self-consistent field (MCSCF) wave functions are required first, then the MRCI wave functions are needed for taking account of the dynamic electron correlation effect, and finally, the size-extensivity correction is needed after the MRCI calculation. The multireference singles and doubles configuration interaction with Davidson size-extensivity correction[25,26] (MR-CISD+Q) is a widely used quantum chemistry ab initio method developed for dealing with the excited states of small molecules. Knowles and Werner[27−29] had performed an internally contracted scheme, in which the rapid increase of the number of configurations with the increase of the size of basis sets can be avoided efficiently.

The main goal of this paper is to study the electronic state structures and the transition properties of the GaBr molecule, especially the effect of SOC, by using the internally contracted MR-CISD+Q method. The 23 Ω states generated from the 12 Λ−S states of GaBr are studied for the first time. Their potential energy curves and the spectroscopic constants are obtained after considering the avoided crossing rule between states of the same point group symmetry. The transition properties of the $A^3\Pi_{0+}-X^1\Sigma^+_{0+}$ and $B^3\Pi_1-X^1\Sigma^+_{0+}$ transitions are predicted for the first time, including the transition dipole moments (TDMs), the Franck−Condon (FC) factors and the radiative lifetimes.

2. Computational Details

All of our calculations are performed with MOLPRO[30] ab initio programs package release 2002.6 on a PC LINUX platform with 2.2 GHz Pentium IV CPU and 1 GB memory. The spectroscopic constants and the FC factors are evaluated by using Le Roy's LEVEL[31] program.

For a series of given bond lengths, the ground state molecule orbitals (MOs) are calculated first by using the spin-restricted Hartree−Fock (RHF) method. Then the state-averaged complete active space MCSCF (CASSCF) calculations are carried out using previous RHF orbitals as starting values for orbital optimization. Utilizing the CASSCF energies as reference values, the energies of the Λ−S states are computed by using the internally contracted MR-CISD+Q method. Gallium and bromine being heavy elements, both their electronic correlation and relativistic effects are expected to be very important. On one hand, the Douglas-Kroll[32,33] scalar relativistic one-electron integrals have been taken into account, and additionally, spin−orbit matrix elements and eigenstates are computed using the Breit-Pauli (BP) operator[34] after electron correlation calculations. The state-interacting method is employed for SOC calculations, which means that the spin−orbit eigenstates are obtained by diagonalizing $\hat{H}_{el} + \hat{H}_{SO}$ on the basis of eigenfunctions of $\hat{H}_{el}$. For MRCI wave functions, the full BP spin−orbit operator is used merely for computing the matrix elements between internal configurations (no electrons in external orbitals); a mean-field one-electron fock operator is employed for contributions of the external configurations. The error caused by this approximation is less than 1 cm^{-1}.[34] Because of the limitation of MOLPRO program package, C_{2v} point group symmetry has been considered for GaBr molecule although it belongs to a higher symmetry group. The numbering of the C_{2v} point group is A1, B1, B2, and A2. The transform relationship between the $C_{\infty v}$ and C_{2v} groups is $\Sigma^+ = A1$, $\Sigma^- = A2$, $\Pi = B1 + B2$, and $\Delta = A1 + A2$. In other words, the Π and Δ states are degenerate in the C_{2v} symmetry. The Π state can be represented by B1 and B2, while the Δ state can be represented by A1 and A2 of C_{2v} symmetry at the same time. All of the 12 valence Λ−S states of GaBr are obtained from the three roots of the A1 representation and the two roots of the B1, B2, and A2 representations of the C_{2v} symmetry, for the singlet and triplet states, respectively. In this total of 18 roots calculated in the C_{2v} symmetry, all roots of the B1 and B2 representations (Π states) and one root of the A1 and A2 representations (Δ states) are degenerate in our calculation. The PECs are plotted by connecting the calculated points with the aid of the avoided crossing rule between electronic states of the same point group symmetry. The spectroscopic constants, including the equilibrium internuclear distance R_e, the harmonic vibrational constants ω_e and $\omega_e\chi_e$, the relative electronic energy referred to the ground state T_e, and the dissociation energy D_e, can be derived by fitting the PECs.

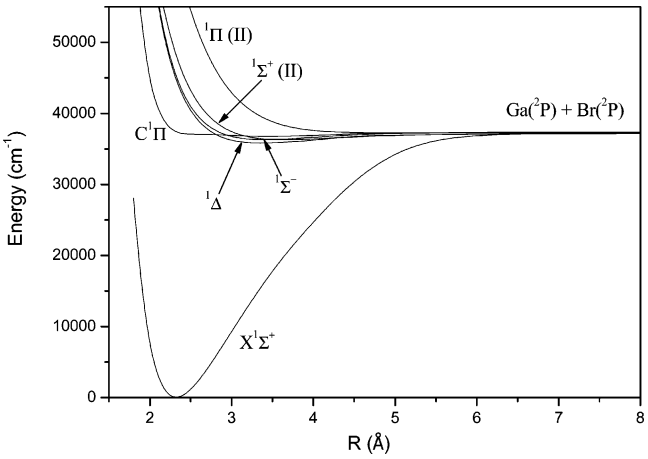

Figure 1. Potential energy curves of the ground and the singlet excited Λ−S states of GaBr.

The entirely uncontracted aug-cc-pVQZ Gaussian all-electron basis sets are used for both atoms (Ga: 22s17p13d3f2g, Br: 22s17p13d3f2g)[35] in the calculations of Λ−S states. Because the SOC is treated as a perturbation for the energies of Λ−S states, and the spin−orbit integral program in the MOLPRO program package is restricted to basis functions with $l_{max} = 3$ (f functions), we therefore use uncontracted cc-pVTZ all-electron basis sets for both atoms (Ga: 20s13p9d1f, Br: 20s13p9d1f)[35] in the SOC calculations. This reduces the computational costs drastically without losing much accuracy. The difference of SOC splitting energies between the calculations using larger and smaller basis sets is less than 2 cm^{-1}.[48] In the CASSCF and subsequent MR-CISD+Q calculations, nine molecular orbitals are selected as active space, which corresponds to the Ga 4s4p5s and Br 4s4p shells. The outermost $4s^24p^1$ electrons of Ga and $4s^24p^5$ electrons of Br are placed in the active space. The 10 electrons in the 3d shell of the Ga atom are used for some core−valence correlations, while the rest of the inner electrons are frozen. That is to say, there are altogether 20 electrons in the correlation energy calculations.

3. Results and Discussion

3.1. Results and Analysis of the Λ−S States. Twelve valence Λ−S states of the GaBr molecule are computed in this paper, which are obtained from the interaction of the ground-state Ga (^{2}P, $4s^24p^1$) with the ground-state Br (^{2}P, $4s^24p^5$). The computed PECs of singlet Λ−S states are shown in Figure 1, while the curves of triplet Λ−S states are plotted in Figure 2. There are eight bound states ($X^1\Sigma^+$, $^3\Pi$, $^3\Sigma^+$, $^1\Delta$, $^3\Delta$, $^1\Sigma^+$(II), $^1\Sigma^-$, and $^3\Sigma^-$) in all of these 12 valence Λ−S states. Their spectroscopic constants are fitted and summarized in Table 1.

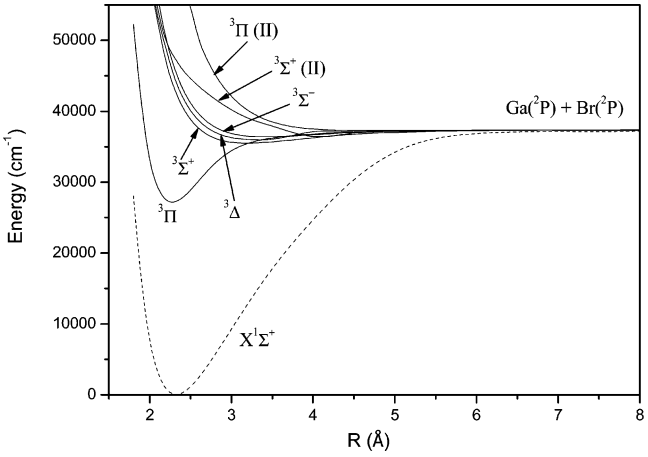

Figure 2. Potential energy curves of the ground and the triplet excited Λ−S states of GaBr.

TABLE 1: Theoretical Spectroscopic Constants of the Bound Valence Λ−S States of GaBr

Λ−S states	T_e (cm^{-1})	R_e (Å)	ω_e (cm^{-1})	$\omega_e\chi_e$ (cm^{-1})	D_e (eV)
$X^1\Sigma^+$	0	2.3536	269.5	0.62	4.377
$^3\Pi$	28437.2	2.2972	272.1	1.48	0.851
$^3\Sigma^+$	34507.8	3.4663	76.8	2.74	0.099
$^1\Delta$	34740.2	3.5663	52.9	1.69	0.070
$^3\Delta$	34863.7	3.5223	71.8	2.89	0.054
$^1\Sigma^+$(II)	35008.4	4.0178	28.2	0.88	0.036
$^1\Sigma^-$	35116.5	3.5972	44.2	1.63	0.023
$^3\Sigma^-$	35171.6	3.5918	47.0	2.13	0.016

The entire 12 valence Λ−S electronic states of the GaBr molecule are dissociated to the ^{2}P (Ga 4p) + ^{2}P (Br 4p) atomic state. By analyzing the compositions of MRCI wave functions, it has been found that the ground-state $X^1\Sigma^+$ is characterized mainly by the closed-shell electronic configuration $1\sigma^2 2\sigma^2 1\pi^4 3\sigma^2 2\pi^0$, where the 1π and 2π MOs are dominated by the *p*-orbitals of bromine and gallium, respectively. For the ground state, the R_e result is only about 0.001 Å greater, the ω_e and $\omega_e\chi_e$ results are only about 3 cm^{-1} greater and 0.1 cm^{-1} less, and the D_e result is only about 0.05 eV higher than experimental values.

There are two states $^3\Pi$ and $^1\Pi$ arising from the first excited electronic configuration $1\sigma^2 2\sigma^2 1\pi^4 3\sigma^1 2\pi^1$. Experimentally, the $A^3\Pi_{0^+}$ and $B^3\Pi_1$ states were found at 28163.2 and 28534.2 cm^{-1},[16] respectively. Our theoretical T_e result of the $^3\Pi$ state is 28437.2 cm^{-1}, between the experimental values of that of the A and B states. The errors of theoretical R_e, ω_e, and $\omega_e\chi_e$ results are less than 0.002 Å, 2 cm^{-1}, and 0.2 cm^{-1}.

In contrast to the deep potential well states of $X^1\Sigma^+$ and $^3\Pi$, some other higher Λ−S states $^3\Sigma^+$, $^1\Delta$, $^3\Delta$, $^1\Sigma^+$(II), $^1\Sigma^-$, and $^3\Sigma^-$, which lie at about 35000 cm^{-1}, have only rather shallow potential wells (D_e < 0.1 eV). Because of their very low vibrational frequencies and fairly large R_e values, it can be predicted that their transition bands to the ground state will overlap each other and form a weak continuum. Miescher[7] had observed some diffuse absorption bands near 36000 cm^{-1}, indicating shallow upper state potential curves, which matches well with our calculated results. In addition to these shallow potential well bound states, four other Λ−S states, $^1\Pi$, $^3\Sigma^+$(II), $^3\Pi$(II), and $^1\Pi$(II), at higher position are repulsive in nature. At the equilibrium bond length of the ground state, their vertical excitation energies are 37746, 46834, 60605, and 60853 cm^{-1}, respectively. Note that all of the excited Λ−S states will cross with each other with the increase of bond length (R > 3 Å). Hence the shapes of their theoretical PECs may become rather different after considering the effects of SOC and the avoided crossing rule between the Ω states of same symmetry.

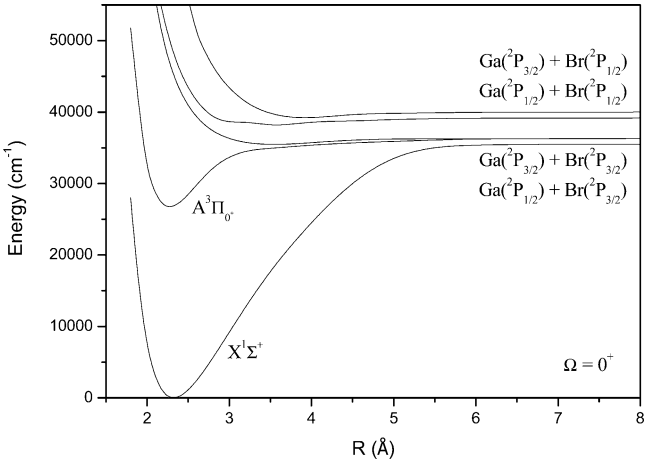

Figure 3. Potential energy curves of the $\Omega = 0^+$ states of GaBr.

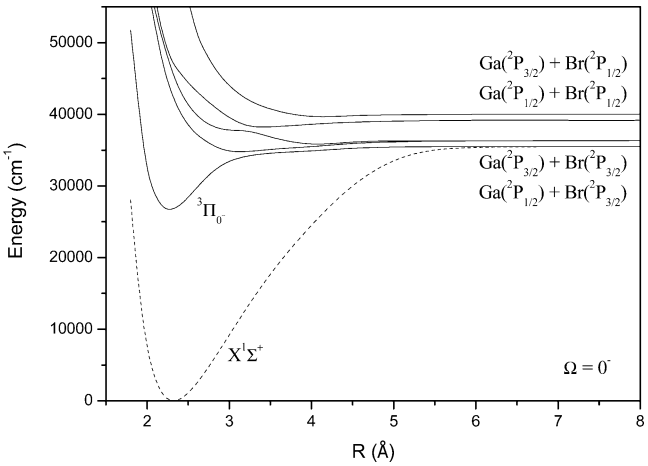

Figure 4. Potential energy curves of the $\Omega = 0^-$ states of GaBr.

TABLE 2: Dissociation Relationships of Valence Ω States of GaBr

		energy (cm^{-1})	
atomic state (Ga + Br)	Ω state	theory	expt.[24]
$^2P_{1/2} + {}^2P_{3/2}$	2, 1, 1, 0^+, 0^-	0	0
$^2P_{3/2} + {}^2P_{3/2}$	3, 2, 2, 1, 1, 1, 0^+, 0^+, 0^-, 0^-	833	826
$^2P_{1/2} + {}^2P_{1/2}$	1, 0^+, 0^-	3657	3685
$^2P_{3/2} + {}^2P_{1/2}$	2, 1, 1, 0^+, 0^-	4490	4511

3.2. Results and Analysis of the Ω States. Once the SOC is introduced into the calculation, different Λ−S states which have common Ω states become mixed. Table 2 shows the dissociation limits for the possible Ω states and the corresponding energy separations. Compared with the Λ−S state calculation results, the ground-state dissociation limit of Ga (^{2}P) + Br (^{2}P) splits into four asymptotes, of which the Ga ($^2P_{1/2}$) + Br ($^2P_{3/2}$) is the lowest. The successively higher dissociation limits are Ga ($^2P_{3/2}$) + Br ($^2P_{3/2}$), Ga ($^2P_{1/2}$) + Br ($^2P_{1/2}$), and Ga ($^2P_{3/2}$) + Br ($^2P_{1/2}$). The calculated atomic energy splittings are 833 ($^2P_{1/2} - {}^2P_{3/2}$ of Ga) and 3657 ($^2P_{3/2} - {}^2P_{1/2}$ of Br), being in good agreement with the observed values of 826 and 3685 cm^{-1},[24] respectively. There are 23 SOC states with $\Omega = 0^+$, 0^-, 1, 2, and 3 being generated from the 12 Λ−S states of GaBr molecule. The PECs of the states of $\Omega = 0^+$, 0^- and 1 symmetries are plotted in Figures 3, 4, and 5, respectively, while the PECs of the states of $\Omega = 2$ and 3 symmetries are drawn in Figure 6.

TABLE 3: Spectroscopic Constants of the Bound Valence Ω States of GaBr

Ω states	T_e (cm^{-1})	R_e (Å)	ω_e (cm^{-1})	$\omega_e\chi_e$ (cm^{-1})	D_e (eV)	dominant Λ−S states at the corresponding R_e (%)
$X0^+$(I)	0	2.3534	267.3	0.71	4.173	$X^1\Sigma^+$(99)
		2.3525[a]	266.7[a]	0.73[a]	4.32[b]	
0^-(I)	28008.7	2.2975	270.8	1.69	0.699	$^3\Pi$(99)
$A0^+$(II)	28043.7	2.2967	271.7	1.61	0.799	$^3\Pi$(99)
	28163.2[a]	2.295[a]	274.3 [a]	1.56[a]		
B1(I)	28395.5	2.3000	269.4	1.68	0.651	$^3\Pi$(99)
	28534.2[a]	2.296[a]	272.0[a]	1.60[a]		
2(I)	28809.9	2.3023	268.1	1.75	0.600	$^3\Pi$(99)
C1(II)	33560.5	3.4847	48.8[c]		0.011	$^3\Pi$(48), $^3\Delta$(33), $^1\Pi$(15)
0^-(II)	33931.9	3.5272	59.6	2.21	0.069	$^1\Sigma^-$(50), $^3\Sigma^+$ (44), $^3\Pi$(5)
2(II)	33951.2	3.1564	64.2	2.77	0.067	$^3\Pi$(73), $^1\Delta$(21), $^3\Delta$(5)
3(I)	33971.3	3.5241	71.5	2.90	0.064	$^3\Delta$(100)
0^+(III)	34225.2	4.0075	26.0	0.81	0.029	$^1\Sigma^+$(II)(61), $^3\Sigma^-$(37), $^3\Pi$(II)(2)
2(III)	34240.6	3.7712	45.1	2.61	0.031	$^3\Delta$(38), $^1\Delta$(34), $^3\Pi$(23),
1(III)	34306.1	3.5679	46.4	4.07	0.023	$^3\Pi$(II)(4), $^1\Pi$(36), $^3\Sigma^-$(31), $^3\Pi$(23), $^3\Sigma^+$(9), $^3\Pi$(II)(1)
0^-(III)	37056.2	3.5002	45.9	1.95	0.030	$^1\Sigma^-$(33), $^3\Pi$(32), $^3\Sigma^+$(23), $^3\Pi$(II)(10)
1(IV)	37079.2	3.5067	52.7	2.86	0.027	$^3\Delta$(57), $^3\Pi$(19), $^1\Pi$(17), $^3\Pi$(II)(6)
0^+(IV)	37381.8	4.2881	38.2	0.03	0.094	$^3\Pi$(II)(89), $^3\Sigma^-$(9), $X^1\Sigma^+$(1)
2(IV)	37575.4	3.4683	79.3	3.53	0.070	$^3\Pi$(36), $^3\Delta$(32), $^1\Delta$(29), $^3\Pi$(II)(2)
1(V)	37774.2	3.5211	51.7	2.02	0.045	$^3\Sigma^-$(34), $^3\Sigma^+$(24), $^1\Pi$(22), $^3\Pi$(15), $^3\Sigma$(II)(4)

[a] Experimental values from ref 16. [b] Experimental values from ref 10. [c] $\Delta G_{1/2} = \omega_e - \omega_e\chi_e$ interval.

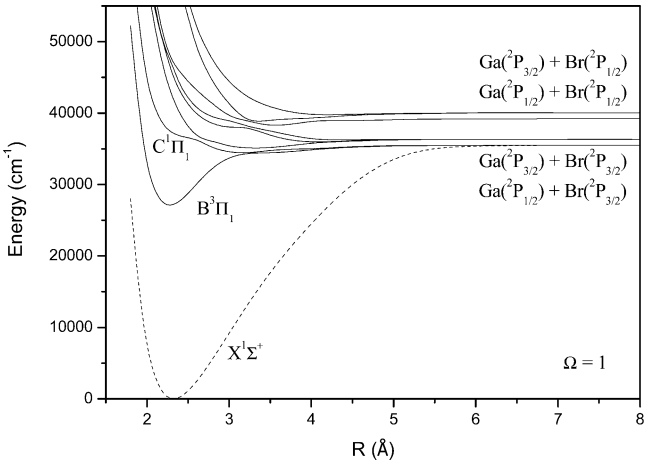

Figure 5. Potential energy curves of the Ω = 1 states of GaBr.

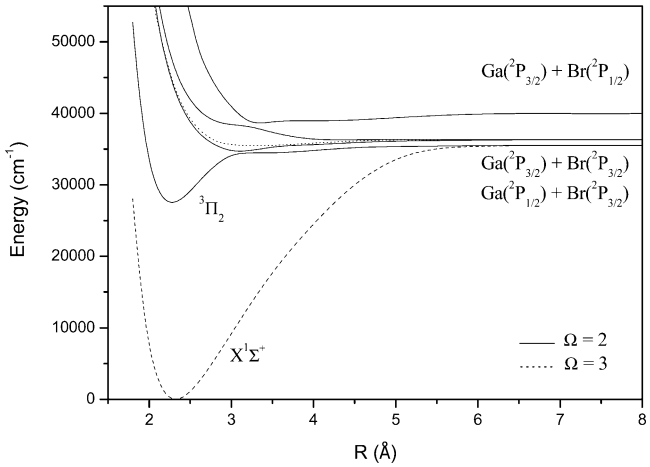

Figure 6. Potential energy curves of the Ω = 2 and 3 states of GaBr.

The spectroscopic constants of bound Ω states and their dominant Λ−S state compositions at R_e are reported in Table 3. With the increasing of bond lengths, the states that have the same Ω components will mix, and the compositions of these bound Ω states will become more complex. For the closed-shell singlet ground-state $X^1\Sigma^+_{0_+}$ that is mainly composed of $X^1\Sigma^+$, the theoretical R_e, ω_e, and $\omega_e\chi_e$ results of the ground state with SOC correction have only a minute improvement. But because of the splittings of atomic ground states of Ga and Br, the theoretical D_e results of the ground state $X0^+$ decrease about 0.2 eV than the $X^1\Sigma^+$ state after considering the SOC.

Four Ω components, namely 0^-, 0^+, 1, and 2 of the $^3\Pi$ state, have potential wells with depth of about 0.8 eV, of which only two have been found experimentally, designated as $A^3\Pi_{0_+}$ and $B^3\Pi_1$. Their energies increase in the order of 0^-, 0^+, 1, and 2 near their equilibrium bond lengths. The calculated energy separations of 0^-(I)−$A0^+$(II) and B1(I)−2(I) are about 35 and 410 cm^{-1}, respectively, while the splitting of $A0^+$(II)−B1(I) is about 350 cm^{-1}, being in good agreement with the corresponding experimental value of 370 cm^{-1}.[16] Compared with the experimental spectroscopic constants of the A and B states, the theoretical results of T_e are only 119.5 and 138.7 cm^{-1} lower, the R_e are only 0.002 and 0.004 Å longer, the ω_e are only 2.6 cm^{-1} smaller, and the $\omega_e\chi_e$ are only 0.05 and 0.08 cm^{-1} greater. For the other two Ω components, their excitation energies are, respectively, 28008.7 and 28809.9 cm^{-1}, and their R_e and ω_e values are rather close to those of the A and B states as well. The transitions from them to the ground state are forbidden and have not been observed in experiment, hence their degrees of agreement are not known.

It may be noted that the excited Λ−S states will cross with each other at the region of 34000−38000 cm^{-1} when the bond length is larger than 3 Å. After considering the SOC, their PEC shapes have been changed dramatically as compared with the pure Λ−S states state as a result of the mixture of them and the avoided crossing rule between Ω states of the same symmetry. Although the $C^1\Pi$ state is repulsive, the C1(II) state has a rather shallow potential well (0.011 eV) lying at 33560.5 cm^{-1} after the effect of SOC is included in calculation. At equilibrium bond length, it is composed of the Ω = 1 component

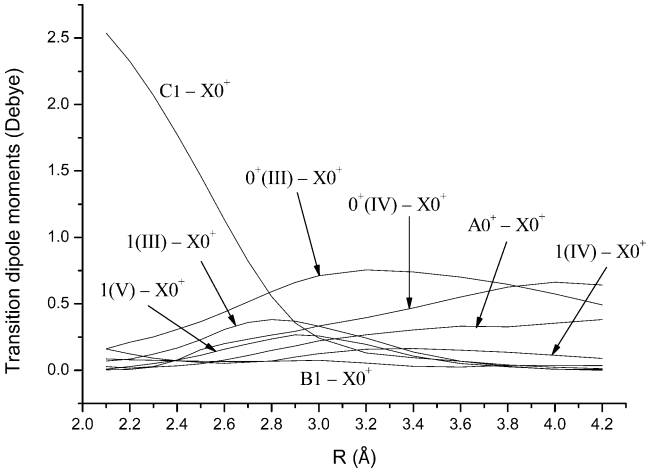

Figure 7. Transition dipole moments of the dipole-allowed bound excited Ω states as functions of the internuclear distance.

TABLE 4: Radiative Lifetimes of the $A^3\Pi_{0_+}$ and $B^3\Pi_1$ States at Lower Vibrational Levels to the Ground-State Transitions

	radiative lifetimes				
transitions	$v'=0$	$v'=1$	$v'=2$	$v'=3$	$v'=4$
$A^3\Pi_{0_+} - X^1\Sigma^+_{0_+}$ (ms)	2.62	2.53	2.44	2.34	2.25
$B^3\Pi_1 - X^1\Sigma^+_{0_+}$ (μs)	252.37	243.22	234.34	224.71	215.32

of $^3\Pi$(48%), $^3\Delta$(33%), and $^1\Pi$(15%) states. Only two vibrational energy levels ($v' = 0$, 1) in the C1(II) state have been found in our calculation. Additionally, some other rather close bound Ω states lying at the region of 34000−38000 cm^{-1} are found (listed in Table 3). Except for the $^3\Delta_3$ state, the SOC makes the PECs and the compositions of each Ω state much more complex, especially for those mixed Ω states resulting from the avoided crossing rule come into being. Hence, it can be concluded that the transitions of these states to the ground state are hard to be observed and analyzed in experiment.

3.3. Transition Properties Analysis. In all of the excited bound Ω states, only the transitions from $A0^+$(II), B1(I), C1(II), 0^+(III), 1(III), 1(IV), 0^+(IV), and 1(V) states to the ground state are dipole-allowed, and only the A and B states had been observed in experiment. Figure 7 shows the computed TDMs of these excited states to the ground $X0^+$(I) state transitions as functions of the internuclear distance. Near the equilibrium bond length of the ground state, the TDM of the C1(II)−$X0^+$ transition are much greater than that of the other transitions, but it decreases rapidly with the increase of bond length.

The radiative lifetime is defined by

$$\tau_{v'} = (\sum_{v''} A_{v'v''})^{-1}$$

where the $A_{v'v''}$ Einstein coefficients represent the emission transition probabilities from the v' state to the v'' stages. Assuming isotropic excitation and unpolarized dipolar radiation, the radiative lifetime can be brought to the expression[36]

$$\tau_{v'} = \frac{3h\epsilon_0 c^3}{16\pi^3}[\sum_{v''}(\Delta E)^3 g_e |\mu_{elec}(v',v'')|^2]^{-1}$$

where g_e is a statistical weight factor which usually equals to unity except for $\Sigma \rightarrow \Pi$ emission; in the latter case $g_e = 2$,[37] ΔE is the transition energy between two vibrational levels, and $\mu_{elec}(v',v'')$ is the TDM between the v' and v'' states (as the higher-order moments are assumed to be negligible). The radiative lifetimes of the $A^3\Pi_{0+}-X^1\Sigma^+_{0_+}$ and $B^3\Pi_1-X^1\Sigma^+_{0_+}$ transitions at lower vibrational levels are computed and listed in Table 4. At $v' = 0$ vibrational level, the radiative lifetime of the $A^3\Pi_{0_+}$ state is of the order of milliseconds, while that of the $B^3\Pi_1$ state is of the order of microseconds.

The intensity distribution in a band system can largely be explained by the FC principle. This can be illustrated by the FC factors assuming that the electronic transition moment does not vary over the band system. The FC factors of the $A^3\Pi_{0_+}-X^1\Sigma^+_{0_+}$ and $B^3\Pi_1-X^1\Sigma^+_{0_+}$ transitions are evaluated by the LEVEL program and are listed in Table 5. It is obviously that the 0−0 bands have the maximum transition probability. Most of our calculated FC factors are rather close to the experimental values.

TABLE 5: Theoretical Franck−Condon Factors of the $A^3\Pi_{0_+}-X^1\Sigma^+_{0_+}$ and $B^3\Pi_1-X^1\Sigma^+_{0_+}$ Transitions[a]

	$v''=0$	$v''=1$	$v''=2$	$v''=3$	$v''=4$	$v''=5$	$v''=6$
				$A^3\Pi_{0_+}-X^1\Sigma^+_{0_+}$			
$v'=0$	0.6418	0.2579	0.0758	0.0191	0.0044	0.0009	0.0002
	(0.52)	(0.27)	(0.047)	(0.0028)	(0.0000)	(0.0000)	(0.0000)
$v'=1$	0.3118	0.2094	0.2793	0.1356	0.0465	0.0133	0.0032
	(0.23)	(0.16)	(0.36)	(0.11)	(0.0085)	(0.0000)	(0.0000)
$v'=2$	0.0443	0.4197	0.0446	0.2181	0.1649	0.0736	0.0253
	(0.068)	(0.25)	(0.028)	(0.36)	(0.17)	(0.016)	(0.0000)
$v'=3$	0.0020	0.1068	0.4222	0.0017	0.1466	0.1697	0.0955
	(0.016)	(0.13)	(0.19)	(0.0000)	(0.31)	(0.22)	(0.024)
$v'=4$	0.0000	0.0062	0.1669	0.3905	0.0056	0.0880	0.1569
	(0.0033)	(0.043)	(0.16)	(0.12)	(0.012)	(0.27)	(0.26)
				$B^3\Pi_1-X^1\Sigma^+_{0_+}$			
$v'=0$	0.6746	0.2404	0.0654	0.0155	0.0034	0.0007	0.0001
	(0.54)	(0.27)	(0.042)	(0.0020)	(0.0000)	(0.0000)	(0.0000)
$v'=1$	0.2901	0.2596	0.2767	0.1214	0.0388	0.0105	0.0024
	(0.23)	(0.18)	(0.36)	(0.097)	(0.0059)	(0.0000)	(0.0000)
$v'=2$	0.0343	0.4128	0.0792	0.2313	0.1528	0.0624	0.0202
	(0.064)	(0.25)	(0.042)	(0.37)	(0.15)	(0.011)	(0.0000)
$v'=3$	0.0010	0.0842	0.4399	0.0148	0.1699	0.1637	0.0828
	(0.015)	(0.12)	(0.20)	(0.0020)	(0.34)	(0.20)	(0.015)
$v'=4$	0.0000	0.0031	0.1337	0.4332	0.0001	0.1146	0.1582
	(0.0030)	(0.039)	(0.15)	(0.14)	(0.0043)	(0.31)	(0.24)

[a] Figures in parentheses refer to experimental values from reference.[16]

4. Conclusions

Internally contracted MR-CISD+Q calculations using entirely uncontracted all-electronic aug-cc-pVQZ basis sets have been performed on the ground and valence excited states of the GaBr molecule. The scalar relativistic correction is taken into account by using Douglas-Kroll one-electron integrals. The spin−orbit matrix elements and eigenstates are computed using the BP operator after electron correlation calculations. The effect of SOC is treated as a perturbation for the energies of Λ−S states. The PECs of all valence states and the spectroscopic constants of bound states are fitted. It is the first time that the entire 23 Ω states generated from the 12 Λ−S states of GaBr molecule are studied in a theoretical way. And finally, the transition properties of the $A^3\Pi_{0+}-X^1\Sigma^+_{0+}$ and $B^3\Pi_1-X^1\Sigma^+_{0+}$ transitions are predicted for the first time. The agreement between our calculation results and available experimental data is very satisfactory. After considering the effect of SOC, the errors of the theoretical T_e, R_e, ω_e, and $\omega_e\chi_e$ results are less than 150 cm^{-1}, 0.005 Å, 3 and 0.1 cm^{-1}.

Calculation results show a series of rather shallow potential well excited states (D_e < 0.1 eV) lying in the region of about 34000−38000 cm^{-1}. The observed diffuse absorption bands near 36000 cm^{-1} can be contributed to the transitions from them to the ground state. Except for the $^3\Delta_3$ state, the SOC makes the PECs and the components of each Ω state much more complex, especially for some mixed Ω states, resulting from the avoided crossing rule come into being. Their transitions to the ground state are hard to observe and analyze. All of these calculation results show that consideration of the SOC effect is absolutely necessarily for the molecules that contain heavy atoms and have shallow potential well electronic states.

The calculations on transition properties show that the radiative lifetime of the $A^3\Pi_{0+}$ state of the GaBr molecule is of the order of milliseconds, while that of the $B^3\Pi_1$ state is of the order of microseconds.

Acknowledgment. This work is supported by the National Natural Science Foundation of China (Project No. 69878010).

References and Notes

(1) [1]Effer, D. *J. Electrochem. Soc.* **1965**, *112*, 1020.
(2) Donnelly, V. M.; Karlicek, R. F. *J. Appl. Phys.* **1982**, *53*, 6399.
(3) Karlicek, R. F.; Hammarlund, B.; Ginocchio, J. *J. Appl. Phys.* **1986**, *60*, 794.
(4) Lane, S. J.; Green, M. *J. Chem. Soc., Faraday Trans.* **1991**, *87*, 995.
(5) Petrikalm, A.; Hochburg, J. *Z. Phys.* **1933**, *86*, 214.
(6) Miescher, E.; Wehrli, M. *Helv. Phys. Acta* **1933**, *6*, 458.
(7) Miescher, E.; Wehrli, M. *Helv. Phys. Acta* **1934**, *7*, 331.
(8) Barrett, A. H.; Mandel, M. *Phys. Rev.* **1958**, *109*, 1572.
(9) Bulewicz, E. M.; Phillips, L. F.; Sugden, T. M. *Trans. Faraday Soc.* **1961**, *57*, 921.
(10) Barrow, R. F. *Trans. Faraday Soc.* **1960**, *56*, 952.
(11) Savithry, T.; Rao, D. V. K.; Murty, A. A. N.; Rao, P. T. *Physica*, **1974**, *75*, 386.
(12) Huber K. P.; Herzberg, G. *Molecular Spectra and Molecular Structure IV: Constants of Diatomic Molecules*; Van Nostrand: Princeton, NJ, 1979; p 222.
(13) Nair, K. P. R.; Pahlmann, H.-U. S.; Hoeft, J. *Chem. Phys. Lett.* **1981**, *80*, 149.
(14) Burnecka, J. B.; Żyrnicki, W. *Physica C* **1980**, *100*, 124.
(15) Burnecka, J. B. *Spectrosc. Lett.* **1990**, *23*, 887.
(16) Burnecka, J. B.; Żyrnicki, W. *Bull. Pol. Acad. Sci. Chem.* **1994**, *42*, 64.
(17) Burnecka, J. B.; Żyrnicki, W. *Chem. Phys. Lett.* **1995**, *238*, 346.
(18) Grabandt, O.; Mooyman, R.; Delange, C. A. *Chem. Phys.* **1990**, *143*, 227.
(19) Venkatasubramanian, R.; Saksena, M. D.; Singh, M. *Chem. Phys. Lett.* **1993**, *210*, 367.
(20) Balasubramanian, K.; Tao, J. X.; Liao, D. W. *J. Chem. Phys.* **1991**, *95*, 4905.
(21) Kim, G. B.; Balasubramanian, K. *J. Mol. Spectrosc.* **1992**, *152*, 192.
(22) Mencone, G.; Tozer, D. J. *Chem. Phys. Lett.* **2002**, *360*, 38.
(23) Yang, X.; Lin, M.; Zou, W.; Zhang, B. *Chem. Phys. Lett.* **2002**, *362*, 190.
(24) Moore, C. E. *Atomic Energy Level*; U. S. National Bureau of Standards: Washington DC, 1971; p 159.
(25) Langhoff, S. R.; Davidson, E. R. *Int. J. Quantum Chem.* **1974**, *8*, 61.
(26) Bruna, P. J.; Peyerimhoff, S. D.; Buenker, R. J. *Chem. Phys. Lett.* **1981**, *72*, 278.
(27) Werner, H.-J.; Knowles, P. J. *J. Chem. Phys.* **1988**, *89*, 5803.
(28) Knowles, P. J.; Werner, H.-J. *Chem. Phys. Lett.* **1988**, *145*, 514.
(29) Knowles, P. J.; Werner, H.-J. *Theor. Chim. Acta* **1992**, *84*, 95.
(30) Werner, H.-J.; Knowles, P. J.; Amos, R. D.; Bernhardsson, A.; Bernhardsson, A.; Berning, A.; Celani, P.; Cooper, D. L.; Deegan, M. J. O.; Dobbyn, A. J.; Eckert, F.; Hampel, C.; Hetzer, G.; Korona, T.; Lindh, R.; Lloyd, A. W.; McNicholas, S. J.; Manby, F. R.; Meyer, W.; Mura, M. E.; Nicklass, A.; Palmieri, P.; Pitzer, R.; Rauhut, G.; Schütz, M.; Schumann, U.; Stoll, H.; Stone, A. J.; Tarroni, R.; Thorsteinsson, T. MOLPRO, a package of ab initio programs designed by H.-J. Werner and P. J. Knowles, ver. 2002.6; 2003.
(31) Le Roy, R. J. *LEVEL, A Computer Program for Solving the Radial Schrödinger Equation for Bound and Quasibound Levels*, University of Waterloo Chemical Physics Research Report CP-642R3, ver. 7.4. 2001.
(32) Douglas, M.; Kroll, N. M. *Ann. Phys.* **1974**, *82*, 89.
(33) Hess, B. A. *Phys. Rev. A* **1986**, *33*, 3742.
(34) Berning, A.; Schweizer, M.; Werner, H.-J.; Knowles, P. J.; Palmieri, P. *Mol. Phys.* **2000**, *98* 1823.
(35) Wilson, A. K.; Woon, D. E.; Peterson, K. A.; Dunning, T. H., Jr. *J. Chem. Phys.* **1999**, *110*, 7667.
(36) Whiting, E. E.; Nicholls, R. W. *Astrophys. J. Suppl.* **1974**, *27*, 1.
(37) Glass-Maujean, M.; Quadrelli, P.; Dressler, K. *J. Chem. Phys.* **1984**, *80*, 4355.